European Journal of Medicinal Chemistry 84 (2014) 77–89

Contents lists available at ScienceDirect

European Journal of Medicinal Chemistry

journal homepage: http://www.elsevier.com/locate/ejmech

Original article

Synthesis and characterization of novel phosphonocarboxylate inhibitors of RGGT

Fraser Coxon [b, 1], Łukasz Joachimiak [a, 1], Arafath Kaja Najumudeen [c, 1], George Breen [b], Joanna Gmach [a], Christina Oetken-Lindholm [c], Rebecca Way [b], James Dunford [d], Daniel Abankwa [c], Katarzyna M. Błażewska [a, *]

[a] Institute of Organic Chemistry, Lodz University of Technology, Żeromskiego 116, 90-924 Łódź, Poland
[b] Musculoskeletal Programme, Institute of Medical Sciences, University of Aberdeen, Foresterhill, Aberdeen AB252ZD, UK
[c] Turku Centre for Biotechnology, Åbo Akademi University, Tykistökatu 6B, 20520 Turku, Finland
[d] University of Oxford, Nuffield Department of Orthopaedics, Rheumatology and Musculoskeletal Sciences, The Botnar Research Center, UK

ARTICLE INFO

Article history:
Received 21 February 2014
Received in revised form
14 June 2014
Accepted 27 June 2014
Available online 28 June 2014

Keywords:
Phosphonocarboxylates
Bisphosphonates
Geranylgeranylation
RGGT
GGPPS

ABSTRACT

Phosphonocarboxylate (PC) analogs of the anti-osteoporotic drugs, bisphosphonates, represent the first class of selective inhibitors of Rab geranylgeranyl transferase (RabGGTase, RGGT), an enzyme implicated in several diseases including ovarian, breast and skin cancer. Here we present the synthesis and biological characterization of an extended set of this class of compounds, including lipophilic derivatives of the known RGGT inhibitors. From this new panel of PCs, we have identified an inhibitor of RGGT that is of similar potency as the most active published phosphonocarboxylate, but of higher selectivity towards prenyl pyrophosphate synthases. New insights into structural requirements are also presented, showing that only PC analogs of the most potent 3rd generation bisphosphonates inhibit RGGT. In addition, the first phosphonocarboxylate-derived GGPPS weak inhibitor is reported.

1. Introduction

Compounds bearing a phosphonocarboxylate (PC) scaffold, in which phosphonate and carboxylate groups are linked via one carbon atom have received considerable attention as potential antiviral [1–3] and anticancer agents [4,5]. They are therefore structurally similar to pyrophosphate, an important endogenous regulator of mineralization, but unlike pyrophosphate they are resistant to hydrolysis.

The interest in nitrogen-containing PCs was initiated during structure–activity relationship (SAR) studies of the well established nitrogen-containing bisphosphonates (BP), which inhibit osteoclast-mediated bone resorption by targeting the mevalonate pathway enzyme farnesyl pyrophosphate synthase (FPPS) (Fig. 1) [6].

The first PC (**1c**, 3-PEHPC, NE-10790), derived from bisphosphonate **2**, in which one phosphonic group was exchanged for a carboxylic group, has no effect on FPPS, but was found to be the first selective inhibitor of RGGT [7], inhibiting osteoclast activity *in vitro* [7], *in vivo* [8] and exhibiting anti-cancer properties both *in vitro* and in an animal model [9,10]. Comparable potency was observed for analogs **1a**–**b** [4]. Much higher potency against RGGT was achieved with the subsequent generation of PCs, compounds **3a**–**c**, derived from BP **4** (Fig. 2) [11,12].

RGGT is responsible for geranylgeranylation of Rab proteins (Fig. 1), the largest family of small GTPases. Both RGGT and Rab proteins have recently been implicated in numerous diseases including cancer, neurological disorders, bacterial and viral infections [13–15]. To date a few classes of RGGT inhibitors have been identified, including PC derivatives of BPs [4,7,11,12], tripeptide analogues [16,17], compounds derived from GGTase 1 inhibitors, with pentasubstituted pyrrolidine analogs [18], compounds

Abbreviations: PC, phosphonocarboxylate; BP, bisphosphonate; RGGT, Rab geranylgeranyl transferase, Rab GGTase, GGTase 2; TAG tunnel, a tunnel adjacent to GGPP binding site in RGGT; FTase, farnesyl transferase; FPPS, farnesyl pyrophosphate synthase, farnesyl diphosphate synthase; GGTase 1, geranylgeranyl transferase 1; NFSI, *N*-fluoro-*N*-(phenylsulfonyl) benzenesulfonamide.

* Corresponding author.
E-mail address: katarzyna.blazewska@p.lodz.pl (K.M. Błażewska).

[1] These authors contributed equally.

http://dx.doi.org/10.1016/j.ejmech.2014.06.062
0223-5234/

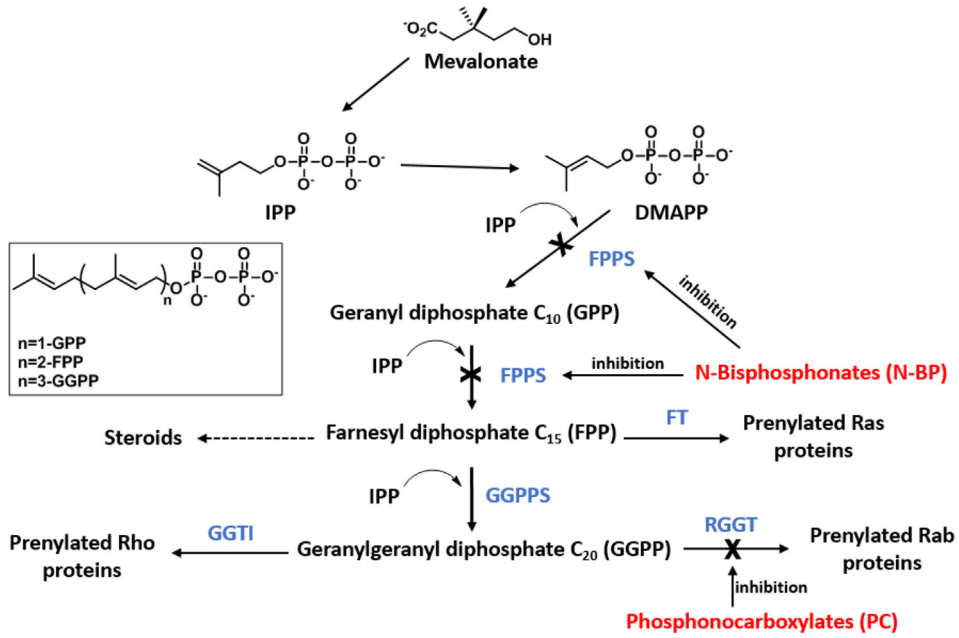

Fig. 1. Mevalonate pathway and transferases responsible for prenylation of selected proteins, including the sites of action of the most potent BPs and PCs (enzymes are shown in blue, inhibitors are shown in red). (For interpretation of the references to colour in this figure legend, the reader is referred to the web version of this article.)

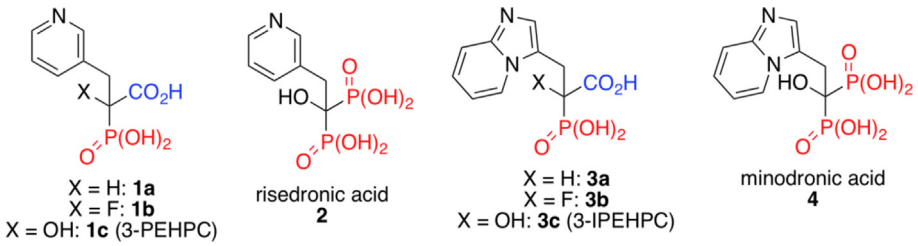

Fig. 2. Structures of the first PC inhibitors of RGGT (**1** and **3**) and the BPs (**2** and **4**) from which they were derived.

derived from FTase inhibitor, based on a tetrahydrobenzodiazepine scaffold [19,20] and triazole-based BPs [21].

The lack of a crystal structure of the RGGT–PC complex limits the possibilities for the rational design of more potent PC inhibitors and therefore further elaboration of the pharmacophore model by synthesizing and evaluating the biological activity of new analogs is required.[2] It has been proposed that PCs interact with the TAG tunnel of RGGT, a tunnel adjacent to the GGPP binding site that is not present in the other prenyl transferases, FTase and GGT-1, making it a promising site for selective targeting of RGGT [17]. The TAG tunnel is thought to accommodate the first GG-cysteine prior to addition of the second geranylgeranyl group, explaining why the PCs inhibit only the second geranylgeranylation step [22].

We based our studies on the trend observed for the PC–BP pairs that have already been investigated (**1**–**2** and **3**–**4**), which implied a possible correlation between structure–activity relationships for inhibition of FPPS by BPs and RGGT by PCs with respect to the nitrogen-containing group.

Therefore, we focused on the synthesis of **5**, the PC analog of the potent 3rd generation heterocyclic BP, zoledronic acid **9**, and PC analogs (**6**–**8**) of the 2nd generation aminoalkyl BPs, pamidronic **10**, alendronic **11** and ibandronic **12** acids (Fig. 3), which are all potent, clinically used BPs. Until now, only analogs bearing a heterocyclic amine side chain have been tested (Fig. 2: **1a**–**c**, **3a**–**c**) [4,7,11,12].

The second group of compounds that we generated were analogs of PCs with reported potency against RGGT (**1c**, **3c**), in which the hydroxyl group was exchanged for an alkyl substituent (Fig. 4). The influence of a hydrophobic substituent that mimics the geranylgeranyl pyrophosphate (GGPP) substrate of RGGT on PC activity has not been studied before. We synthesized five analogs of 3-PEHPC (**1d**–**h**), modified with alkyl chains of different lengths and one analog of 3-IPEHPC (**3g**). We expected that an increase in the hydrophobicity of the PCs might result in increased activity due to the inhibitor fitting into the GGPP binding pocket and/or improved cell permeability [23].

2. Results

2.1. Chemistry

A variety of approaches to the synthesis of PCs have been described. They include formation of C–P bond, via introduction of phosphonic group either in the Arbuzov–Michaelis reaction of trialkyl phosphite with α-bromoesters [24], or in a reaction of enolate and chlorodialkyl phosphite [25], or reaction of diethyl phosphite with α-ketoester [11]. In other methods the carboxylic moiety is introduced into the carbon adjacent to the phosphonate

[2] Even though the crystal structures of RGGT with other inhibitors were solved, attempts to dock newly designed PCs into enzyme did not give coherent results.

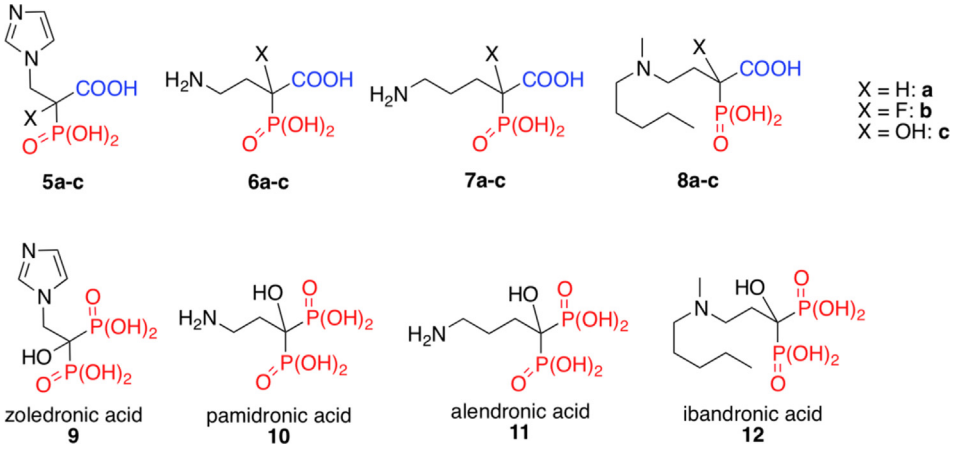

Fig. 3. Structures of novel PC analogs (**5**–**8**) derived from the second and third generation BPs (**9**–**12**) (as discussed in the Results, structures of PC derivatives containing hydroxy substituent (X = OH, **5**–**8c**) were not synthesized).

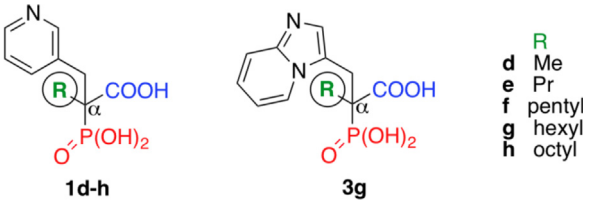

Fig. 4. Structures of analogs of known PC inhibitors of RGGT, modified in position C-α with lipophilic chains (in circles, marked in green) of different lengths. (For interpretation of the references to colour in this figure legend, the reader is referred to the web version of this article.)

group using lithium alkylphosphonate and diethyl carbonate [26] or CO_2 [27]. Yet another approach is based on alkylation of trialkyl phosphonoacetate [27,28] or functionalization of trialkyl 2-phosphonoacrylate via Michael-type addition [5,29,30]. Up to now few examples of nitrogen-containing PCs have been generated [4,11,12].

Our first attempts were directed at the synthesis of PCs with the hydroxyl group retained in the molecule (Fig. 3, compounds **5**–**8c**). We considered two routes for construction of such derivatives, either reaction of dialkyl phosphite with appropriate α-ketoester (an approach successfully applied in the synthesis of **1c** and **3c**) [11,31] or by opening an epoxide ring with an appropriate nucleophile in easily available ethyl 2-(diethoxyphosphoryl)oxirane-2-carboxylate [32]. Both approaches failed; the first route due to problems with obtaining precursory α-ketoesters, the second route due to phosphonate–phosphate rearrangement [33], that could not be suppressed.

BPs and PCs have different SARs regarding the presence of the hydroxyl group. Exchange of the hydroxyl for a hydrogen or halogen atom in BPs leads to a significant decrease of activity against FPPS [4]. By contrast, the analogous switch in PCs has smaller effect on the ability to inhibit Rab prenylation [4,12]. This characteristic was crucial for our efforts, as it enabled us to change the target PCs from hydroxy- (**5**–**8c**) into desoxy- (**5**–**8b**) and fluoro- (**5**–**8c**) analogs. The fluorine atom is considered bioisosteric to C–H, C=O and C–OH groups [34] and its role in molecules of pharmacological use is gaining in importance [35–37].[3]

[3] Also, analogs bearing hydroxyl group may reversibly form dimer complex with boron on exposure with borosilicate glassware [38].

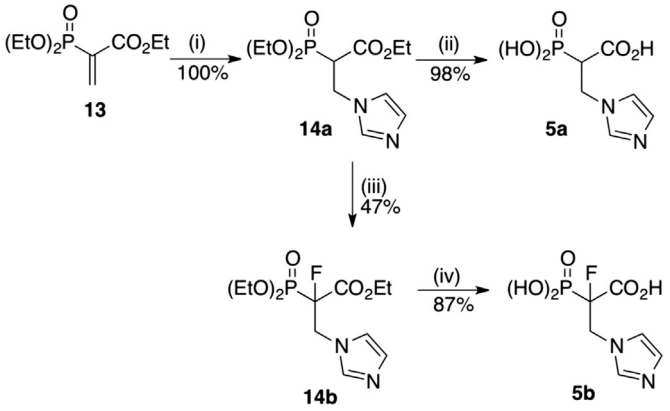

Scheme 1. Synthesis of PC analogs of zoledronic acid. Conditions and reagents: (i) imidazole (1.02 eq), $CHCl_3$, 10 min, rt; (ii) 12 M HCl, reflux; (iii) NaH (1.7 eq), Selectfluor (1.5 eq), THF, 0 °C to rt, 1.25 h; (iv) 12 M HCl, reflux.

The target compounds' structural diversity required separate approaches to synthesise precursory esters. Subsequent fluorination of esters was carried out using either Selectfluor, according to a procedure used previously for fluorination of other PCs [4,12,39], or using *N*-fluoro-*N*-(phenylsulfonyl) benzenesulfonamide (NFSI), according to a procedure applied for fluorination of selected BPs [40]. Fluorination yields were affected by the susceptibility of the products to decomposition, as a result of P–C bond cleavage under basic conditions [32,39]. Free acids were obtained upon hydrolysis using 12 M HCl under reflux.

Triester **14a** was obtained via Michael-type addition of imidazole to easily available **13** [29,32,41] (Scheme 1). The reaction was immediate (a few minutes) and quantitative. Due to the compound's instability (see Supporting information for details), we immediately subjected it to hydrolysis (98%) or fluorination (47%).

Precursors of **6a** and **7a** were obtained by applying the Arbuzov reaction (Scheme 2). Appropriate α-bromoesters **17** and **18** were synthesized from γ- or δ-amino acids **15** and **16**. *N*-Phthalyl products were brominated in the alpha position [42], and subjected to reaction with triethyl phosphite, producing triester precursors **19a** and **20a** with 82–100% yields. Fluorination of esters gave products **19b** and **20b** with 49% yields. Free acids **6a**–**b** and **7a**–**b** were obtained upon acidic hydrolysis with 66–85% yields.

Compound **7a** could be also obtained by alkylation of **21** with **22** (Scheme 3). However, when *t*-BuOK was used as a base, conversion

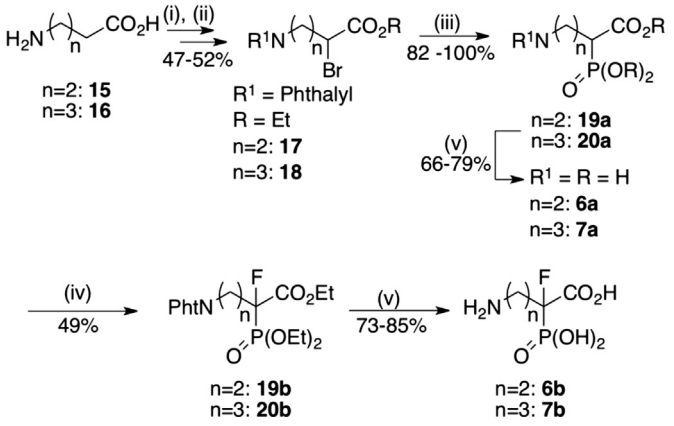

Scheme 2. Synthesis of PC analogs of pamidronic and alendronic acids. Conditions and reagents: (i) phthalic anhydride (1.02 eq), 180 °C, 35 min; (ii) $SOCl_2$ (5 eq), CCl_4, 1.25 h reflux, then NBS (1.2 eq) with HBr(aq) (cat), 1.1 h, reflux, then EtOH; (iii) $P(OEt)_3$ (1.92 eq), 165 °C, 4 h; (iv) NaH (1.7 eq), Selectfluor (1.5 eq), THF, 0 °C to rt, 1.25 h; (v) 12 M HCl, reflux.

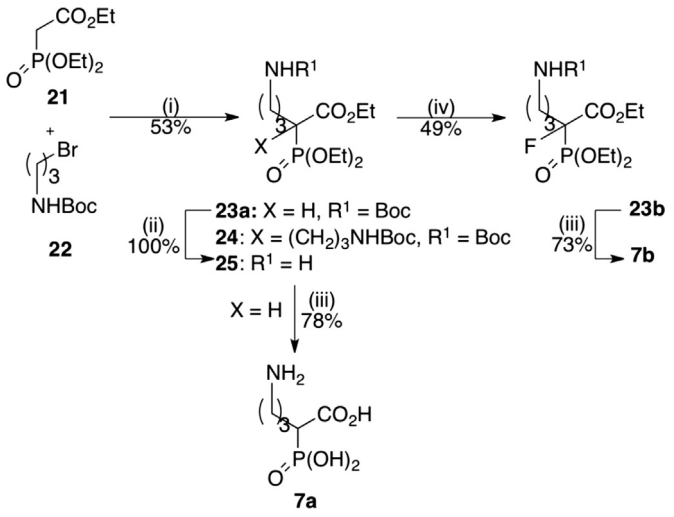

Scheme 3. Synthesis of PC analogs of pamidronic acid: second method. Conditions and reagents: (i) *t*-BuOK (2.2 eq), THF, 5 d, rt; (ii) 3 M HCl (g)/EtOH, 1 h 40 min, rt; (iii) 12 M HCl, reflux; (iv) NaH (1.7 eq), Selectfluor (1.5 eq), THF, 1.25 h, 0 °C to rt.

did not exceed 70%. Higher conversion was achieved under different conditions (using different bases, solvents and PTC catalysts), but then it was compromised by lower selectivity, yielding also the product of dialkylation **24**.[4] Triester **23a** was fluorinated with 49% yield.

The synthesis of **8a** was based on introducing a carboxyester group to the phosphonate **26** (Scheme 4) [26]. Subsequently, the acetal moiety was hydrolysed to produce aldehyde **28** which was subjected to reductive amination with *N*-methyl-*N*-penthylamine [44]. Hydrolysis of **29a** led to the expected product **8a**. Fluorination of **29a** with Selectfluor gave a mixture of unidentified products. Efforts to overcome this limitation by fluorination of precursory **27** or **28** failed. Application of *N*-fluoro-*N*-(phenylsulfonyl)

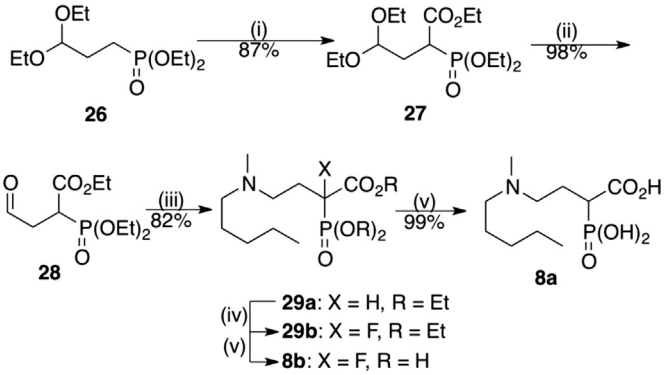

Scheme 4. Synthesis of PC analogs of ibandronic acid. Conditions and reagents: (i) LDA (2.2 eq), THF, hexane, −78 °C, then $(EtO)_2CO$ (1 eq), to rt, 20 h; (ii) 80% AcOH, 60 °C, 3 h; (iii) *N*-methyl-*N*-penthylamine (0.9 eq), $NaBH(OAc)_3$ (0.9 eq), DCM, 4 h, rt; (iv) 1.6 M BuLi, NFSI; (v) 12 M HCl, reflux.

benzenesulfonamide (NFSI) [40] led to the fluorination product **29b** with 50% yield. The free acid **8b** was obtained with 90% purity.

A second group of compounds, modified with a lipophilic chain (Scheme 5), was synthesized by the alkylation reaction of **30** with picolyl chloride or with chloro-2-methyl-imidazo[1,2-a]pyridine.[5]

Synthesis of the α-alkyl phosphonoacetate **30** was achieved using the Arbuzov reaction [24], giving compounds in gram quantities and 61–71% yields. Alternatively, alkylation of **21** with alkyl bromide can be applied, but this approach invariably gives a mixture of **30**, substrate and the product of dialkylation, impeding product isolation.

The analogs **30** thus obtained were subjected to alkylation with picolyl chloride (Scheme 5), using conditions reported previously for alkylation of triethyl phosphonoacetate with benzyl-like chlorides [4,12] and α-alkyl phosphonoacetate with allyl bromide [26], giving pure products in 19–56% after column chromatography. Optimization efforts did not improve this process. Free acids **1** were obtained upon hydrolysis of **31** with 32–72% yields.

Synthesis of α-alkylated analogs of 3-IPEHPC proved more challenging. In the alkylation reaction, we either observed **30g**–**h** recovery or the expected triester **32g**–**h** in low yields 11–14%. The free acid **3g** was synthesized with 93% purity.

These novel PCs were evaluated for their ability to inhibit RGGT, other prenyl transferases and/or mevalonate pathway enzymes in intact cells, which has the advantage over isolated enzyme assays of assessing the cellular availability of the compounds at the same time. Two complementary and independent techniques were used.

2.2. Biological evaluations

2.2.1. Biological activity testing using Rab-NANOPS

In order to test the biological activity of the compounds, we used a recently described cell-based FRET-assay that allows for the detection of functional membrane anchorage of lipid-modified proteins [45,46]. Three FRET-biosensors that report on steady-state protein farnesylation (Ras-NANOPS), as well as RGGT-dependent geranylgeranylation of dual- (Rab5-NANOPS) and mono-prenylated Rab proteins (Rab8-NANOPS) were first used to determine the potency of compounds at 500 μM.

We found that three compounds, **5a**, **5b** and **1h** significantly reduced the FRET-signal of Rab5-NANOPS (Fig. 5A), but not of Ras-

[4] Synthesis of the compound **23a** was reported in patent [43], using NaH in THF. No product of dialkylation was reported. In contrast, according to our studies conditions reported therein were giving mixture of starting compound with **23a** and dialkylation product **24**.

[5] The introduction of alkyl chain into scaffold containing heterocyclic ring, was expected to be inferior, due to the possibility of forming *N*-alkylation side product.

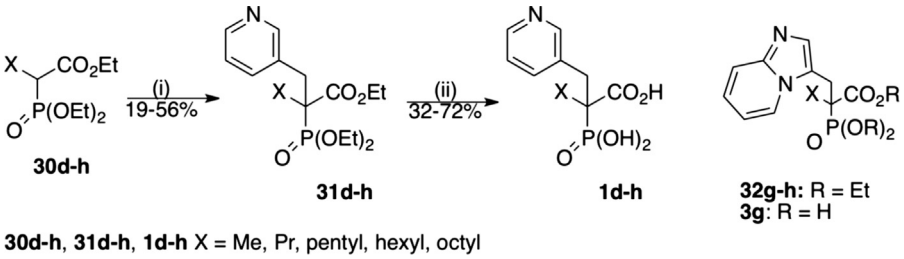

Scheme 5. Synthesis of PC analogs of selected BPs modified with alkyl chain in C-α position. Conditions and reagents: (i) picolyl chloride (1 eq), NaH (3.15 eq), DMF/THF; (ii) 12 M HCl, reflux.

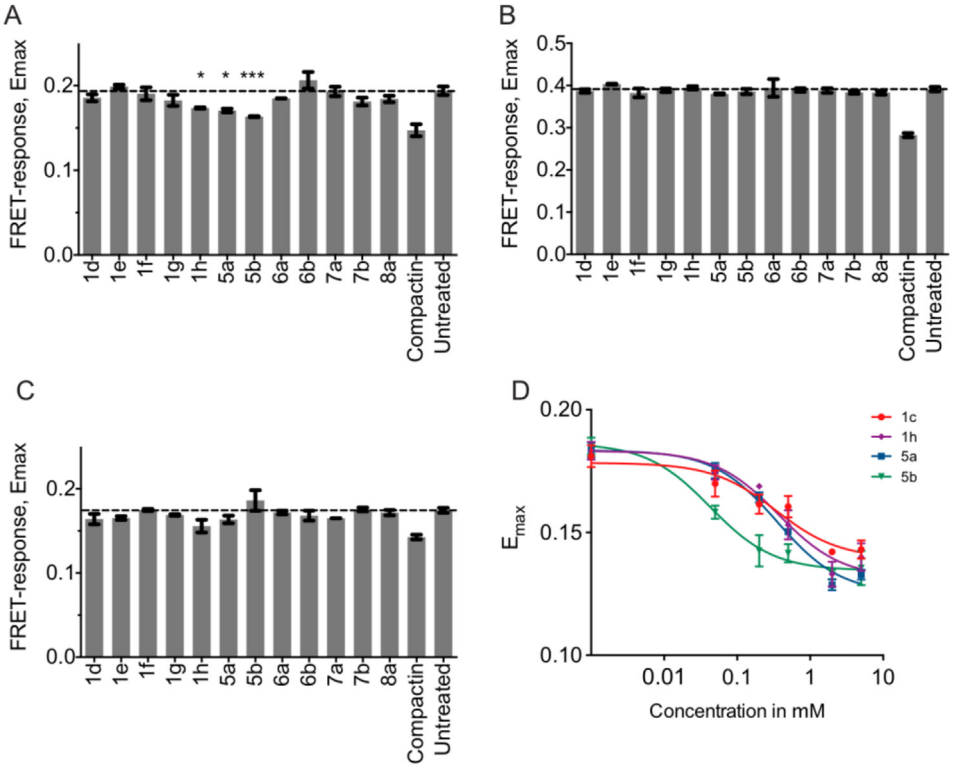

Fig. 5. Cell-based activity testing of PC analogs using FRET-biosensors. (A) BHK21 were transfected with Rab5-NANOPS and screened with the indicated PC analogs at a final concentration of 500 μM for 24 h. The E_{max} values describe the cellular FRET-response of the indicated inhibitors as described in Experimental section. A decrease in the FRET reports on loss of membrane anchorage, cellular redistribution or perturbed nanoclustering of the biosensors. Dotted line indicates the average E_{max} of the non-treated control. Data are presented as mean E_{max} ± s.e.m ($n = 3$): (*) $p < 0.05$ (***) $p < 0.001$ indicate statistical significance vs. non-treated control using one-way ANOVA followed by Dunnett's test as described in Experimental Section. (B and C) FRET-response data like in (A) of Ras- and Rab8-NANOPS, respectively. Treatment with compactin (5 μM), a HMG-CoA inhibitor that blocks synthesis of isoprenoids and therefore protein prenylation, serves as a positive control and reduces the E_{max} value significantly in A–C. (D) Dose–response curves of the effect of **5a**–**5b**, **1c** and **1h** on the E_{max} values of Rab5-NANOPS expressed in BHK cells ($n = 6$).

Table 1
Effect of active PC compounds on prenylation of Rab11 and Rap1a, cell viability in Hela cells, response of FRET-NANOPS. LED = lowest effective dose for inhibition of prenylation.

Compound	Reduction of Hela cell viability (IC_{50}/μM)	Inhibition of Rab11 prenylation (LED/μM)	Inhibition of Rap1A prenylation (LED/μM)	FRET-response of NANOPS[c]			
				Rab5a (IC_{50}/μM)	Rab21 (IC_{50}/μM)	Rab8a (IC_{50}/μM)	Ras (IC_{50}/μM)
8a	No effect	1000	1000	No effect[b]	No effect[b]	No effect[b]	No effect[b]
1c	>2000	250	No effect	630 ± 300	1060 ± 500	No effect[b]	No effect[b]
1h	No effect	500	500	360 ± 60	980 ± 180	No effect[b]	No effect[b]
5a	650	25	No effect	360 ± 40	253 ± 45	No effect[b]	No effect[b]
5b	850	10	No effect	40 ± 3	72 ± 1	No effect[b]	No effect[b]
3c	500	25	400[a]	n.d.	n.d.	n.d.	n.d.
4	1	0.25	0.25	n.d.	n.d.	n.d.	n.d.
9	2.5	0.25	0.25	n.d.	n.d.	n.d.	n.d.

[a] LED for inhibition of Rap1A prenylation in J774 cells [11].
[b] No effect at concentrations 500 and 1000 μM.
[c] Detection specificity: Rab5a and Rab21: dual prenylation and inhibition of RGGT; Rab8a: mono prenylation and inhibition of RGGT; Ras: inhibition of farnesylation and/or palmitoylation.

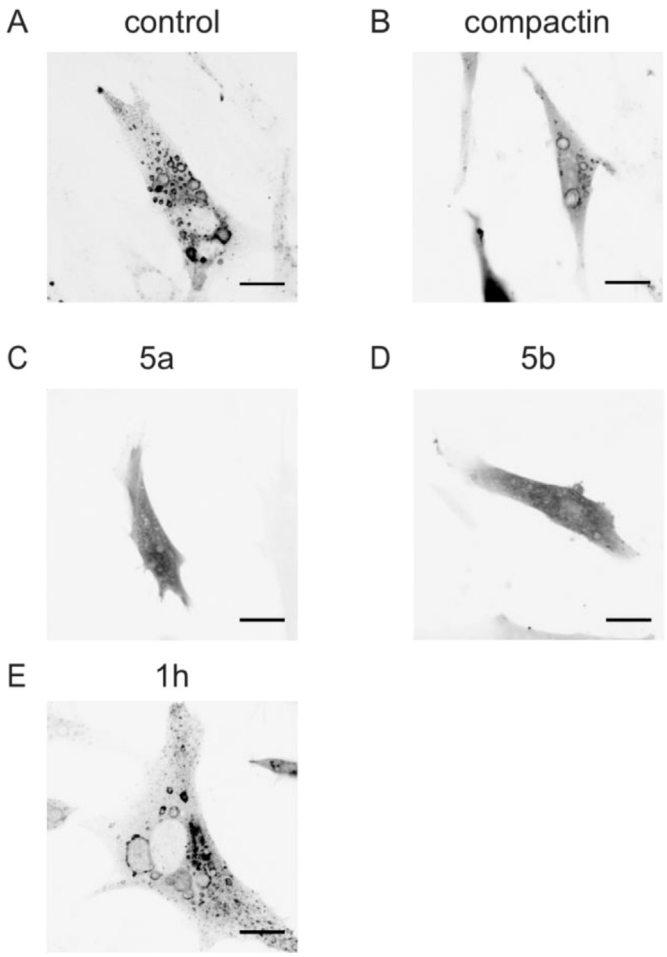

Fig. 6. PC analogs mislocalize Rab5aQ79L in BHK cells. BHK cells expressing mCitrine tagged Rab5aQ79L (i.e. the acceptor of the Rab5-NANOPS FRET-pair) were treated with (A) PBS (control), (B) compactin (5 μM), (C) **5b**, (D) **5a**, (E) **1h** (all three at 500 μM). Following treatment, cells were fixed and imaged using a confocal microscope. Shown are representative images from 2 independent experiments. Scale bars are representative for all images and corresponds to 20 μm.

NANOPS or Rab8-NANOPS (Fig. 5B, C). Analysis with an additional Rab-biosensor for dual-geranylgeranylated Rab proteins, Rab21-NANOPS, confirmed exactly the activity of the identified three compounds (Supporting information: Fig. S108). Dose response analysis with Rab5-NANOPS revealed IC_{50} – values of 360 ± 40 (for **5a**), 40 ± 3 (for **5b**) and 360 ± 60 μM (for **1h**) (Fig. 5D, Table 1).

We next tested what effect these compounds have on the subcellular distribution of the dual-prenylated Rab5. To this end we expressed constitutively active Rab5aQ79L that was N-terminally tagged with the fluorescent protein mCitrine in BHK21 cells and monitored its localization in the cell using confocal microscopy. This Rab5-construct localized to well recognizable hyperfused endosomes (Fig. 6A). However, treatment with compactin led to a strong cytoplasmic redistribution (Fig. 6B). Both **5a** and **5b** completely relocalized the Rab5-construct to the cytoplasm, consistent with a potent inhibition of its prenylation (Fig. 6C, D). On the other hand, **1h** leads to a redistribution of the construct to perinuclear structures and more punctate labelling of endosomes (Fig. 6E).

2.2.2. Biological testing in Hela cells

The novel PCs were also assessed for their ability to inhibit RGGT and/or mevalonate pathway enzymes in intact cells by assaying for the unprenylated forms of Rab11 and Rap1A, which are modified with geranylgeranyl groups by RGGT and GGTase 1, respectively; inhibition of Rab11 prenylation alone is indicative of a specific RGGT inhibitor, while inhibition of prenylation of both GTPases at similar concentrations is indicative of a GGPPS or FPPS inhibitor (see Fig. 1). In addition, we assessed the ability of these PCs to reduce the viable cell number in cultures of Hela cells as a separate indicator of inhibition of prenylation, since inhibition of prenyl transferases or mevalonate pathway enzymes is known to reduce cell viability [7,47–49].

As expected, the first reported PC inhibitor of RGGT, **1c**, weakly inhibited prenylation of Rab11, while bisphosphonate **9** inhibited prenylation of both Rab11 and Rap1A, consistent with its known ability to inhibit FPPS (see Fig. 1) [7,47]. Consistent with the FRET assay, among the first group of synthesized compounds (Fig. 3) compounds **5a**–**b** showed inhibition of RGGT (Fig. 7).

PC analogues of pamidronic and alendronic acids, **6a**–**b** or **7a**–**b**, did not inhibit prenylation of Rab11 or Rap1A in Hela cells at concentrations up to 1 mM, indicating that they do not inhibit RGGT or enzymes of the mevalonate pathway that are involved in prenylation (Fig. 8). Accordingly, only **5a**–**b** analogs reduce Hela cell viability, correlating well with the effects on Rab11 prenylation (Fig. 9C, Table 1), while compounds **6a**–**b** and **7a**–**b** had no effect on the viable cell number of Hela cells after 72 h of treatment with up to 2 mM (Fig. 9A).

The similarity in potency between **5a**–**b** and **3c** for reducing Hela cell viability suggests that the possible weak inhibition of GGPPS by 3-IPEHPC (**3c**) [11] does not significantly contribute to its cellular toxicity, despite the evidence that inhibition of prenylation of other geranylgeranylated proteins (i.e. those modified by GGTase I) has a more profound effect on cell viability than RGGT inhibition [7,50]. In agreement with this, weak inhibition of GGPPS by **1h** (discussed later) also had no effect on the viability of Hela cells (Fig. 9B). The correlation between the inhibition of Rab prenylation

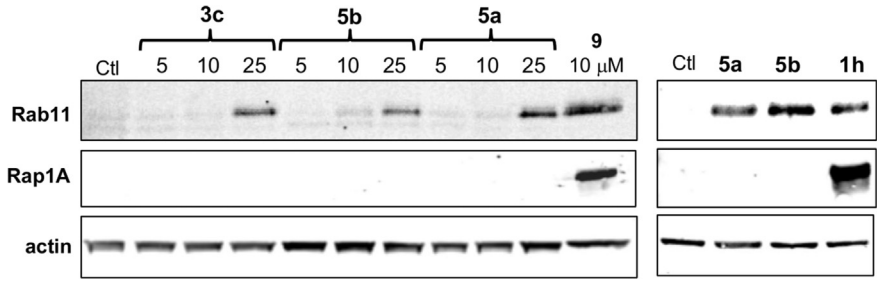

Fig. 7. Effect of zoledronic acid analogues **5a**–**b** on protein prenylation in Hela cells. Hela cells were treated for 48 h with the indicated concentration of PCs (mM); (on the left) or with 0.5 mM **5a**, **5b** or 1 mM **1h** (on the right). Cells were then lysed and the prenylated and unprenylated proteins separated using triton X-114 fractionation. Aqueous phases containing unprenylated proteins were separated by electrophoresis and western blotted for Rab11, Rap1A or actin.

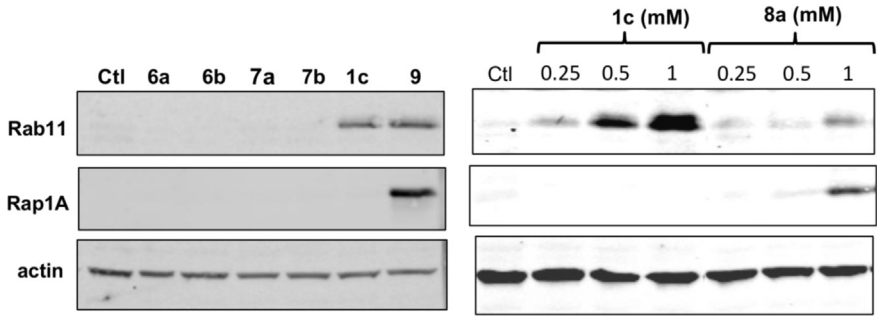

Fig. 8. Effect of desoxy- and fluoro-analogues of alkyl PCs on protein prenylation in Hela cells. Hela cells were treated for 48 h with the indicated PCs (1 mM unless otherwise stated). Cells were then lysed and the prenylated and unprenylated proteins separated using triton X-114 fractionation. Aqueous phases containing unprenylated proteins were separated by electrophoresis and western blotted for Rab11, Rap1A or actin.

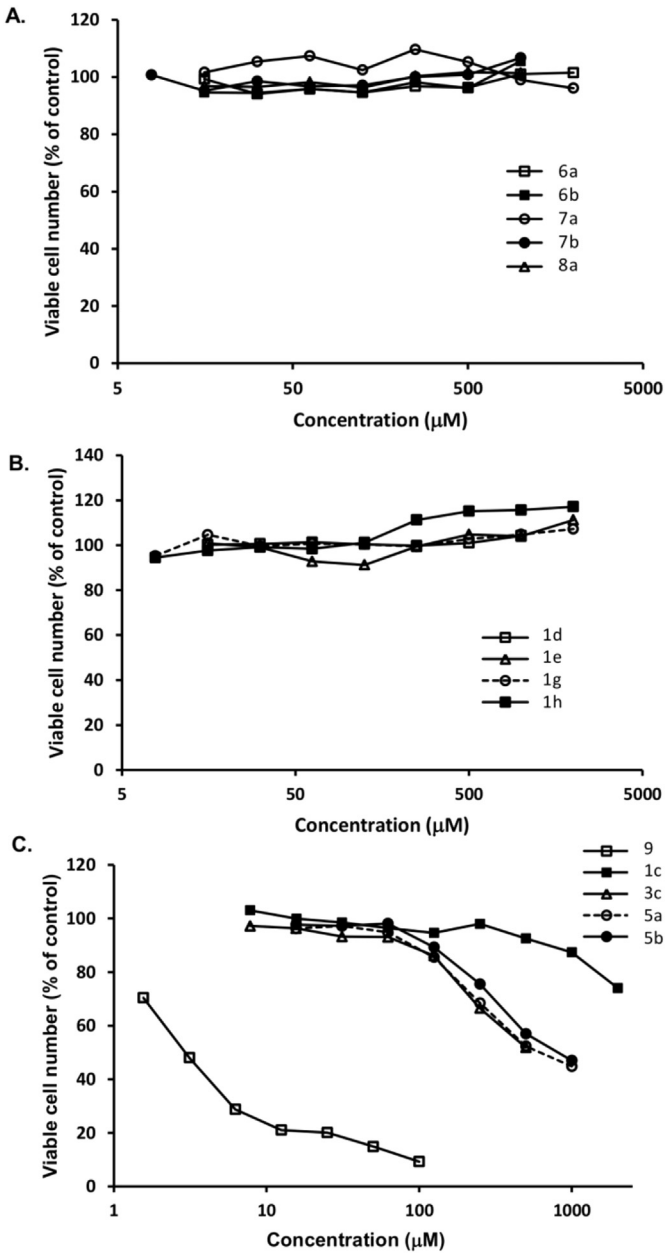

Fig. 9. Effect of PCs on Hela cell viability. Hela cells were treated with PCs for 72 h, then the viable cell number was determined by the Alamar blue assay. Data are the mean from 4 independent experiments.

and reduction of Hela cell viability also indicates that the effects of these novel compounds on viability are due to inhibition of Rab prenylation, and not due to other unrelated cellular effects. Similar results for these compounds were found in RAW264 macrophages, demonstrating that the effects are not cell type specific (data not shown).

Compound **8a**, the PC analog of another 2nd generation bisphosphonate, ibandronic acid (**12**), inhibited prenylation of both Rab11 and Rap1A at 1 mM (Table 1). This suggests that rather than inhibiting RGGT, this compound may inhibit an enzyme of the mevalonate pathway such as GGPPS or FPPS (see Fig. 1). However, the low potency of this compound is reflected in Hela cell viability assays, in which it had no effect at up to 2 mM (Fig. 9A).

Several analogues of 3-PEHPC in which the hydroxyl group was exchanged for an alkyl substituent were tested for biological activity. As in the FRET assay the shorter chain analogues, (C1: **1d**, C3: **1e** and C6: **1g**) were all inactive at up to 1 mM (both Rab11 and Rap1A prenylation). However, the octyl (C8) analogue **1h**, inhibited both Rab11 and Rap1A prenylation at 1 mM, but not at 0.25 mM or lower concentrations (Fig. 10, Table 1). This data suggests that, similar to **8a**, this novel PC does not inhibit RGGT but inhibits either GGPPS or FPPS. Alternatively, it is possible that both RGGT and GGTase I could be inhibited at similar concentrations by both of these PCs.

To exclude the latter possibility, we determined the ability of replenishing cells with GGPP to overcome the inhibition of prenylation; since GGPP is downstream of GGPPS/FPPS it should rescue the effect of inhibitors of these enzymes, but not the effect of RGGT or GGTase I inhibitors (see Fig. 1) [11,51]. Indeed, we found that neither inhibition of Rab11 prenylation by 3-PEHPC (a RGGT inhibitor) nor inhibition of Rap1A prenylation by GGTI-298 (a GGTase I inhibitor) could be rescued by GGPP (Fig. 11A, B). By contrast, inhibition of prenylation of both these proteins by zoledronic acid **9** (an FPPS inhibitor), **1h** or **8a** could be completely prevented by GGPP, indicating that these PCs are possibly GGPPS or FPPS inhibitors. In isolated enzyme assays, we found that **1h** dose-dependently inhibited GGPPS activity (IC_{50} 127 μM), however **8a** had no effect at up to 1 mM (Fig. 11C), implying that it likely targets FPPS instead. At high concentrations, 3-IPEHPC (**3c**) also appears to inhibit GGPPS, although this compound is also a very potent inhibitor of RGGT [11].

3. Discussion

The cellular assays identified two PC analogs as potent and specific inhibitors of RGGT (**5b** > **5a**) (Table 1). **5b** was as potent as 3-IPEHPC (**3c**), which is the most potent PC inhibitor of RGGT yet identified. However, **5b** is more selective, since at high

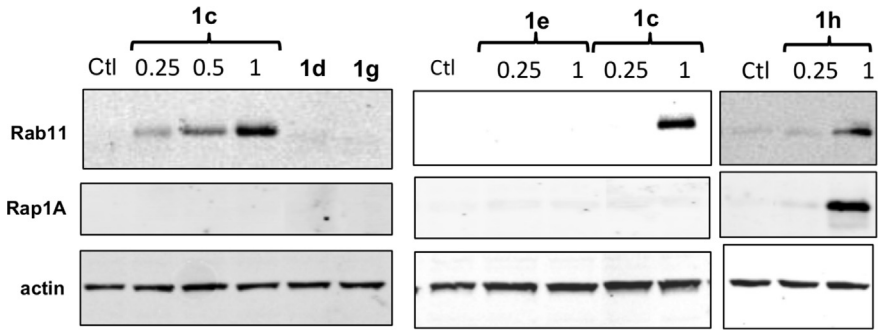

Fig. 10. Effects of alkyl chain length in 3-PEHPC (**1d**, **e**, **g**, **h**) on protein prenylation in Hela cells. Hela cells were treated for 48 h with the indicated PCs (concs in mM; 1 mM unless otherwise stated). Cells were then lysed and the prenylated and unprenylated proteins separated using triton X-114 fractionation. Aqueous phases containing unprenylated proteins were separated by electrophoresis and western blotted for Rab11, Rap1A or actin.

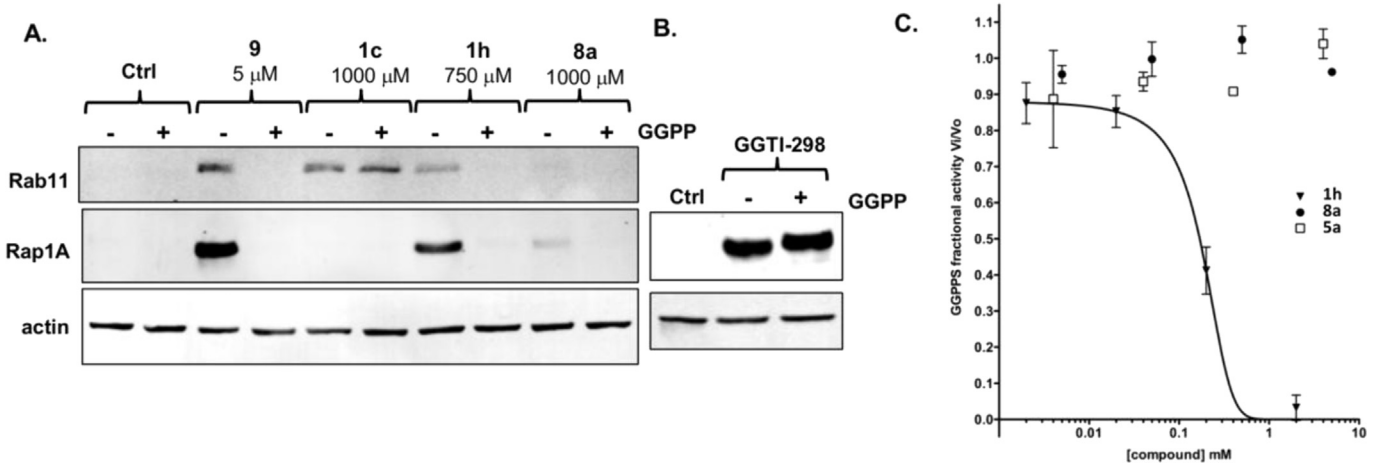

Fig. 11. (A, B) **1h** and **8a** likely inhibit GGPPS in Hela cells. Hela cells were treated with PCs or 10 μM GGTI-298 for 48 h in the presence or absence of 15 μM GGPP. Cells were then lysed and the prenylated and unprenylated proteins separated using triton X-114 fractionation. Aqueous phases containing unprenylated proteins were separated by electrophoresis and western blotted for Rab11, Rap1A or actin. (C) The effect of **5a**, **8a**, **1h** on activity of the GGPPS in an isolated enzyme assay. 40 nM GGPPS was preincubated for 10 min with compounds before initiation of the reaction by addition of substrate. Data represents the mean ± SEM ($n = 3$). Compound **1h** is a weak inhibitor of GGPPS.

concentrations **3c** also inhibits Rap1a prenylation, most likely due to inhibition of GGPPS [11].

The cell-based FRET-assays clearly showed that **5a** and **5b** both significantly decreased the membrane localization of dual-geranylgeranylated Rabs, but not of monoprenylated Rab8 or farnesylated H-Ras derived polypeptide. This observation is consistent with previous studies that reported PCs as inhibitors of the second geranylgeranylation reaction catalysed by RGGT [22].

Interestingly, of all the PCs tested here, those that are analogues of a heterocyclic BP (3rd generation bisphosphonate: **9**) appear to be active RGGT inhibitors (as all previously reported PC inhibitors of RGGT, **1a**–**c** and **3a**–**c**), whereas analogues of the alkyl BPs (2nd generation BPs: **10**, **11**, **12**) appear to be inactive in this respect. Such difference in activity between these two groups of compounds may reflect the difference in the nitrogen character. All active derivatives (**1a**–**c**, **3a**–**c**, **5a**–**b**) have a nitrogen atom in the aromatic ring, at the same distance from the phosphonic group. Also, the most potent representatives of PCs (**5a**–**b** and **3a**–**c**) contain two nitrogen atoms within a differentially substituted imidazole ring. The activity order between **5a** (desoxy-analogue) and **5b** (fluoro-analogue) is broadly in agreement with our previous studies of desoxy and halogen-substituted PC analogues, in which fluoro-derivatives **1b** and **3b** were from 2 to 10 times more potent than their desoxy counterparts [4,12]. It is unclear whether **5b** would be more potent than **5c** (a compound that has yet to be synthesized); other fluoro-PC analogues that we have studied are of similar potency to their parent PCs [4,12].

Increasing hydrophobicity by introducing an alkyl moiety on the branching carbon atom between the phosphonic and carboxylic groups, C-α, completely abolished the ability of 3-PEHPC to inhibit RGGT in Hela cells. This result extends the previously observed trend [4,12], where the desoxy analogs **1a** and **3a**, modified with the smallest possible hydrophobic substituent, a hydrogen atom, were slightly less potent than other studied compounds (**1b**–**c** and **3b**–**c**). Therefore, the presence of a polar group in this position seems to be important for inhibition of RGGT by PCs.

Interestingly, **1h**, which has a C8 side chain shows weak activity against an enzyme of the mevalonate pathway, GGPPS, which accommodates a C15-chain substrate and C20-chain product. This structural trend corresponds well with literature data for alkylated bisphosphonate-derived GGPPS inhibitors.[6] The ibandronic acid

[6] According to Oldfield [52,53] the activity of monoalkylated hydroxy bisphosphonates against GGPPS increases with the length of the side chain, with the C9 chain analogues being the most potent. Of the doubly alkylated analogs, those with two octyl groups showed significant activity against GGPPS. In addition, Wiemer [54] reported that a risedronic acid derivative, with the hydroxyl group exchanged for a geranyl group possessed activity against GGPPS.

analogue, **8a**, is most likely a weak inhibitor of FPPS in Hela cells, since no effect on GGPPS activity could be detected.

Based on the above we expected **1h** to affect the monogeranylgeranylated Rab8-NANOPS biosensor, since deficiency in GGPP should impair prenylation of both mono- and di-geranylgeranylated Rabs. However, only a non-significant effect was observed, which is consistent with the weak potency of the compound. However, an alternative possibility could be ascribed to the fact that FPP can also serve as a substrate for RGGT [55,56,59], and in this case inhibition of GGPPS would cause an increase in FPP, which might then be utilised for prenylation of Rab8 (and other Rab proteins).

The inhibition of prenylation was confirmed by the disrupted subcellular localization of the dual-prenylated Rab5aQ79L. Both **5a**, **5b** significantly mislocalize Rab5aQ79L to the cytosol, while **1h** leads to mistargeting of Rab5a to perinuclear structures. Complete cytosol mislocalization induced by **5a**–**b** may be supporting a hypothesis that RGGT and monoprenylated (but dual-cysteine) Rabs form a dead end complex in the presence of PC, thus depleting cells of RGGT for prenylation of newly synthesized Rabs [22]. On the other hand, the Rab5aQ79L-decorated perinuclear structures detected in cells treated with **1h** resemble those seen with C-terminal mono-cysteine mutants of Rab5a [57], which occurs because monoprenylation of normally diprenylated proteins leads to their mislocalization to ER [58]. We therefore speculate (as suggested in the previous paragraph) that when GGPPS is inhibited, Rab8 is monoprenylated with a farnesyl group by RGGT [59].

4. Conclusions

In summary, we have developed simple routes for the synthesis of novel PC analogs of anti-resorptive bisphosphonates, which were predicted to extend the library of PC-type inhibitors of RGGT. Indeed, biological evaluation of the compounds identified two analogs of zoledronic acid, **5a** and **5b**, to be highly effective RGGT inhibitors in intact cells, with **5b** more potent than **5a** and of comparable potency and higher selectivity to the most potent and selective PC inhibitor of RGGT reported thus far. Interestingly, a PC analogue containing an 8-carbon side chain was found to have no effect on RGGT, but to be a weak inhibitor of GGPPS. Further studies on the synthesis and biological evaluation of new phosphonocarboxylate analogs derived from the most promissing RGGT inhibitors found here, **5a** and **5b**, are in progress.

5. Experimental section

NMR spectra were measured at 250.13 or 700 MHz for ^{1}H NMR, 62.90 or 170 MHz for ^{13}C NMR, 101.30 MHz for ^{31}P NMR, 235.31 MHz for ^{19}F NMR. Chemical shifts (δ) are reported in parts per million (ppm) relative to: in ^{1}H NMR: internal residual $CHCl_3$ in $CDCl_3$ (δ 7.26), or internal residual HDO in D_2O (pH ~ 12, δ 4.76); in ^{31}P NMR: external 85% H_3PO_4 (0 ppm); in ^{13}C NMR: $CDCl_3$ (77.00 ppm); in case of solutions in D_2O signals from residual solvents were used as reference (EtOH (15.17 and 58.13) or acetone (30.89 and 215.94 ppm); in ^{19}F NMR: 70% $CFCl_3$ in $CDCl_3$ (0 ppm). All mass spectra were recorded on the Finnigan MAT 95 double focussing (BE geometry) mass spectrometer (Finnigan MAT, Bremen, Germany). Elemental analyses were performed on a CHNS Elemental Analyser – Elementar Vario MICRO. For final compounds' (**1** and **5**–**8**) precipitation the following solvents were used: water, ethanol, acetone. Only in case of **3g**, diethyl ether was used.

For prenylation studies, PCs were dissolved in calcium-free PBS at stock concentrations of 20–50 mM, and the pH adjusted to 7.6. Compounds were stored at 4 °C prior to use. FPP and GGPP in methanol:ammonia (Sigma) were air-dried to remove most of the solvent, then adjusted to a concentration of 2 mM using DMEM. GGTI-298 (Sigma) was dissolved in 10 mM dithiothreitol in DMSO to give a stock concentration of 10 mM, and stored at −20 °C.

5.1. Chemistry: general procedure for acidic hydrolysis

5.1.1. 3-(1H-imidazol-1-yl)-2-phosphonopropanoic acid (*5a*)

Compound **14a** (1.29 g) was dissolved in 12 M HCl (30 mL). After 5 h reflux it was evaporated to dryness and precipitated using absolute ethanol (7 mL). Precipitate was filtered off and rinsed with minute amounts of ethanol, giving 0.935 g of product. **^{31}P NMR** (D_2O, pH 8): 9,72; **^{1}H NMR**: 3.12 (ddd, $^{2}J_{HP}$ = 21.40, $^{3}J_{HH}$ = 12.10, $^{3}J_{HH}$ = 3.45, CHP, 1H), 4.40 (ddd, $^{2}J_{HH}$ = 13.90, $^{3}J_{HP}$ = 5.35, $^{3}J_{HH}$ = 3.35, CHHCHP, 1H), 4.60 (ddd, $^{2}J_{HH}$ = 13.90, $^{3}J_{HP}$ = 4.15, $^{3}J_{HH}$ = 12.10, CHHCHP, 1H), 7.13–7.14 (m, CH_{ar}, 1H), 7.30–7.31 (m, CH_{ar}, 1H), 7.97 (bs, CH_{ar}, 1H); **^{13}C NMR**: 47.90 (s, CH_2CHP, 1C), 49.34 (d, $^{1}J_{CP}$ = 112.25, CHP, 1C), 120.33 (s, CH_{ar}, 1C), 122.56 (s, CH_{ar}, 1C), 135.92 (s, CH_{ar}, 1C), 172.92 (d, $^{2}J_{CP}$ = 5.65, C(O), 1C). **Elemental analysis**: $C_6H_9N_2O_5P$ Calculated: C 32.74, H 4.12, N 12.73; Found: C 32.89, H 4.37, N 12.57; **Yield**: 98% (0.92 g).

5.1.2. 2-Fluoro-3-(1H-imidazol-1-yl)-2-phosphonopropanoic acid (*5b*)

^{31}P NMR (D_2O, pH 5): 8.10 (d, $^{2}J_{PF}$ = 66.85 Hz); **^{19}F NMR**: 169.27 (d, $^{2}J_{PF}$ = 66.85); **^{1}H NMR**: 4.68–4.90 (signal overlapping with water, CHHN, 1H), 5.01 (ddd, $^{3}J_{HF}$ = 32.50, $^{3}J_{HP}$ = 3.80, $^{2}J_{HH}$ = 15.0, CHHN, 1H), 7.44–7.49 (m, $2H_{ar}$), 8.73–8.75 (m, $1H_{ar}$); **^{13}C NMR**: 53.20 (dd, $^{2}J_{CP}$ = 8.10, $^{2}J_{CF}$ = 20.20, CH_2N, 1C), 96.79 (dd, ^{1}J = 143.95, 196.20 Hz, CFP, 1C), 120.14 (s, C_{ar}), 123.61 (s, C_{ar}), 136.28 (s, C_{ar}), 172.02 (d, ^{2}J = 20.70 Hz, C=O); **Elemental analysis**: $C_6H_8FN_2O_5P$ Calculated: C 30.27, H 3.39, N 11.76; Found: C 30.15, H 3.20, N 11.38. **Scale**: 0.406 g (**14b**); **Yield**: 87% (0.26 g).

5.1.3. 4-Amino-2-phosphonobutanoic acid (*6a*)

^{31}P NMR (D_2O, pH 8): 18.58; **^{1}H NMR**: 1.95–2.25 (m, CH_2CH, 2H), 2.61 (ddd, $^{2}J_{HP}$ = 21.40, $^{3}J_{HH}$ = 9.70, 4.65, CHP, 1H), 3.02 (bt, $^{3}J_{HH}$ = 7.90, CH_2NH_2, 2H); **^{13}C NMR**: 24.67 (d, $^{2}J_{CP}$ = 3.25, CH_2CH, 1C), 37.24 (d, $^{3}J_{CP}$ = 15.90, CH_2NH_2, 1C), 46.80 (d, $^{1}J_{CP}$ = 117.40, CHP, 1C), 177.21 (d, $^{2}J_{CP}$ = 2.25, C(O)OEt); **Elemental analysis**: $C_4H_{10}NO_5P$, Calculated: C 26.24, H 5.50, N 7.65; Found: C 26.14; H 5.58; N 7.62; **Scale**: 0.38 g (**19a**); **Yield**: 79%.

5.1.4. 4-Amino-2-fluoro-2-phosphonobutanoic acid (*6b*)

^{31}P NMR (D_2O, pH 7): 10.84 (d, $^{2}J_{PF}$ = 75.75 Hz); **^{19}F NMR**: −167.96 (d, $^{2}J_{PF}$ = 75.75); **^{1}H NMR**: 2.30–2.63 (m, CH_2CF, 2H); 3.02–3.23 (m, CH_2NH_2, 2H); **^{13}C NMR**: 32.56 (d, ^{2}J = 21.20, CH_2CF, 1C), 36.40 (dd, ^{3}J = 9.95, 4.85, CH_2NH_2, 1C), 98.20 (dd, $^{1}J_{CP,CF}$ = 189.20, 147.95, CPF, 1C), 175.94 (d, ^{2}J = 20.20, C(O)OH, 1C). **Elemental analysis**: $C_4H_9FNO_5P(C_2H_5OH)_{0.43}$ Calculated: C 26.42, H 5.28; Found: C 26.58, H 5.47; **Scale**: 0.396 g (**19b**); **Yield**: 85%.

5.1.5. 5-Amino-2-phosphonopentanoic acid (*7a*)

^{31}P NMR (D_2O, pH 1): 17.44; **^{1}H NMR**: 1.70–2.06 (m, $CHCH_2CH_2$, 4H), 2.88 (ddd, $^{2}J_{HP}$ = 22.35, $^{3}J_{HH}$ = 10.20, $^{3}J_{HH}$ = 3.70, CHP, 1H), 3.03 (bt, $^{3}J_{HH}$ = 7.25, CH_2NH_2, 2H); **^{13}C NMR**: 22.22 (d, J = 3.80, CH_2, 1C), 23.96 (d, J = 14.45, CH_2, 1C), 37.16 (s, CH_2NH_2, 1C), 44.96 (d, $^{1}J_{CP}$ = 120.10, CHP, 1C), 172.92 (d, $^{2}J_{CP}$ = 4.95, COOH, 1C); **Elemental analysis**: $C_5H_{12}NO_5P(HCl)_{0.8}$ Calculated: C 26.54, H 5.70, N 6.19; Found: C 26.68; H 5.78; N 6.30; **Yield**: 66% (from **20a**, scale: 0.30 g) or 78% (from **23a**, scale: 0.276 g).

*5.1.6. 5-Amino-2-fluoro-2-phosphonopentanoic acid (**7b**) (from **23b**)*

^{31}P NMR (D_2O, pH 2): 10.39 (d, $^2J_{PF}$ = 74.35 Hz); **^{19}F NMR**: −176.96 (d, $^2J_{PF}$ = 75.10); **^{1}H NMR**: 1.61–1.98 (m, CH_2CH_2, 2H), 2.09–2.45 (m, CH_2CH_2, 2H), 3.06 (bt, $^3J_{HH}$ = 7.40, CH_2NH_2, 2H); **^{13}C NMR**: 21.86 (dd, $J_{CP,CF}$ = 10.25, 3.65, CH_2CH_2, 1C), 30.76 (d, J = 20.40, CH_2CH_2, 1C), 39.70 (s, CH_2NH_2, 1C), 97.48 (dd, $^1J_{CP,CF}$ = 147.95, 189.65, CFP, 1C), 173.64 (bdd, $^2J_{CP,CF}$ = 24.05, 2.95, C(O), 1C); **Scale**: 0.17 g (**23b**); **Yield**: 73%.

*5.1.7. 4-(Methyl(pentyl)amino)-2-phosphonobutanoic acid (**8a**)*

^{31}P NMR (D_2O, pH 1): 17.99; **^{1}H NMR**: 0.86–0.91 (m, $CH_3(CH_2)_4$, 3H), 1.28–1.36 (m, $(CH_2)_2$, 4H), 1.62–2.38 (m, CH_2, 2H), 2.79–3.00 (m, CHP, 1H), 2.87 (s, CH_3N, 3H), 3.03–3.39 (m, CH_2NCH_2, 4H); **^{13}C NMR**: 11.20 (s, CH_3CH_2, 1C), 19.64, 21.34, 26.01 (3s, $3CH_2$, 3C), 21.65 (d, $^2J_{CP}$ = 8.75, PCHCH_2, 1C), 37.52 (s, CH_3N, 1C), 46.66 (d, $^1J_{CP}$ = 118.59, CHP, 1C), 54.14, 54.38 (s, d, CH_2NCH_2, 2C), 177.22 (d, $^2J_{CP}$ = 4.60, COOH, 1C); **Scale**: 0.087 g (**29a**); **Yield**: 100%.

*5.1.8. 2-Fluoro-4-(methyl(pentyl)amino)-2-phosphonobutanoic acid (**8b**)*

^{31}P NMR (D_2O, pH 2): 7.89 (d, $^2J_{PF}$ = 72.5 Hz); **^{1}H NMR** 0.88 (t, $^3J_{HH}$ = 6.8 Hz, $CH_3CH_2CH_2$, 3H); 1.23–1.38 (m, $CH_3(CH_2)_3CH_2$, 6H); 2.48–2.72 (m, CH_2CHP, 2H), 2.87 (s, CH_3N, 3H); 2.99–3.53 (m, CH_2NCH_2, 4H). **Scale**: 0.10 g (**29b**). Yield: 100% (purity > 80%).

*5.1.9. 2-Methyl-2-phosphono-3-(pyridin-3-yl)propanoic acid (**1d**)*

^{31}P NMR (D_2O, pH 6): 25.59; **^{1}H NMR** (700 MHz): 1.12 (d, $^3J_{HP}$ = 14.6, CH_3C, 3H), 2.84 (dd, $^3J_{HP}$ = 8.7, $^2J_{HH}$ = 13.4, PyCHHC, 1H), 3.48 (dd, $^3J_{HP}$ = 6.6, $^2J_{HH}$ = 13.4, PyCHHC, 1H), 7.40 (dd, $^3J_{HH}$ = 7.9, 4.9, $CH_{Ar\,(5)}$, 1H), 7.72 (dt, $^3J_{HH}$ = 7.9, $^4J_{HH}$ = 1.7, $CH_{Ar\,(4)}$, 1H), 8.36 (bd, $^3J_{HH}$ = 1.7, $CH_{Ar\,(2)}$, 1H), 8.39 (bdd, $^3J_{HH}$ = 4.9, $^4J_{HH}$ = 1.7, $CH_{Ar\,(6)}$, 1H); **^{13}C NMR** (700 MHz): 16.98 (s, CH_3C, 1C), 38.45 (d, $^2J_{CP}$ = 2.3, PyCH$_2$C, 1C), 50.32 (d, $^1J_{CP}$ = 121, C, 1C), 123.74 (s, $CH_{Ar\,(5)}$, 1C), 134.90 (d, $^3J_{CP}$ = 15.6, $C_{Ar\,(3)}$, 1C), 138.93 (s, $CH_{Ar\,(4)}$, 1C), 146.48 (s, $CH_{Ar\,(6)}$, 1C), 149.72 (s, $CH_{Ar\,(2)}$, 1C), 180.64 (s, C=O, 1C). **Elemental analysis**: $C_9H_{12}NO_5P(EtOH)_{0.02}(HCl)_{0.1}$ Calculated: C 43.48, H 4.93, N 5.61; Found: C 43.21; H 4.73; N 5.58; **Scale**: **31d** (0.55 mmol); **Yield**: 47%.

*5.1.10. 2-Phosphono-2-(pyridin-3-ylmethyl)pentanoic acid (**1e**)*

^{31}P NMR (D_2O, pH 13): 18.11; **^{1}H NMR**: 0.89 (t, $^3J_{HH}$ = 7.2, $CH_3(CH_2)_2$, 3H), 1.33–1.51 (m, $CH_3CH_2CH_2$, 2H), 1.59–1.97 (m, $CH_3CH_2CH_2$, 2H), 3.29–3.50 (m, PyCH$_2$C, 2H), 7.95 (dd, $^3J_{HH}$ = 8.0, 4.8, $CH_{Ar\,(5)}$, 1H), 8.55–8.62 (m, CH_{Ar}, 2H), 8.49 (m, $CH_{Ar\,(2,6)}$, 2H), 8.76 (s, CH_{Ar}, 1H); **^{13}C NMR**: 11.93 (s, $CH_3(CH_2)_2$, 1C), 16.15 (d, $^3J_{CP}$ = 5.1, $CH_3CH_2CH_2$, 1C), 28.37 (s, $CH_3CH_2CH_2$, 1C), 33.13 (d, $^2J_{CP}$ = 3.1, PyCH$_2$C, 1C), 51.82 (d, $^1J_{CP}$ = 122.7, C, 1C), 124.41 (s, $CH_{Ar\,(5)}$, 1C), 136.83 (s, $CH_{Ar\,(4)}$, 1C), 137.24 (d, $^3J_{CP}$ = 8.3, $C_{Ar\,(3)}$, 1C), 140.63 (s, $CH_{Ar\,(6)}$, 1C), 147.18 (s, $CH_{Ar\,(2)}$, 1C), 174.70 (s, C=O, 1C); **Elemental analysis**: $C_{11}H_{16}NO_5P$ Calculated: C 48.36, H 5.90, N 5.13; Found: C 48.12, H 6.03, N 5.09; **Scale**: **31e** (0.3 mmol, 0.1 g); **Yield**: 32%.

*5.1.11. 2-Phosphono-2-(pyridin-3-ylmethyl)heptanoic acid (**1f**)*

^{31}P NMR (D_2O, pH 10.7): 22.80, **^{1}H NMR**: 0.74 (t, $^3J_{HH}$ = 7.2, $CH_3(CH_2)_4$, 3H), 1.02–1.32 (m, $CH_3(CH_2)_3(CH_2)_2$, 6H), 1.46–1.59 (m, $CH_3(CH_2)_3CH_2$, 2H), 2.96 (dd, $^3J_{HP}$ = 9.2, $^2J_{HH}$ = 14.0, PyCHHC, 1H), 3.47 (dd, $^3J_{HP}$ = 7.4, $^2J_{HH}$ = 14, PyCHHC, 1H), 7.30 (dd, $^3J_{HH}$ = 8.0, 4.9, $CH_{Ar\,(5)}$, 1H), 7.76 (dt, $^3J_{HH}$ = 7.9, $^4J_{HH}$ = 1.8, $CH_{Ar\,(4)}$, 1H), 8.28 (bdd, $^3J_{HH}$ = 4.9, $^4J_{HH}$ = 1.8, $CH_{Ar\,(6)}$, 1H), 8.37 (m, $CH_{Ar\,(2)}$, 1H); **^{13}C NMR**: 11.63 (s, $CH_3(CH_2)_4$, 1C), 20.10, 30.59, 30.78 (3s, $CH_3CH_2CH_2CH_2CH_2$, 3C), 23.23 (d, $^3J_{CP}$ = 4.5, $CH_3(CH_2)_2CH_2CH_2$, 1C), 34.90 (s, PyCH$_2$C, 1C), 53.03 (d, $^1J_{CP}$ = 116.6, C, 1C), 121.67 (s, $CH_{Ar\,(5)}$, 1C), 134.90 (d, $^3J_{CP}$ = 13.7, $C_{Ar\,(3)}$, 1C), 137.21 (s, $CH_{Ar\,(4)}$, 1C), 144.02 (s, $CH_{Ar\,(6)}$, 1C), 148.12 (s, $CH_{Ar\,(2)}$, 1C), 179.86 (s, C=O, 1C). **Elemental analysis**: $C_{13}H_{20}NO_5P$ Calculated: C 51.83, H 6.69, N 4.65; Found: C 51.58, H 6.66, N 4.54: **Scale**: **31f** (0.2 mmol), **Yield**: 72%.

*5.1.12. 2-Phosphono-2-(pyridin-3-ylmethyl)octanoic acid (**1g**)*

^{31}P NMR (D_2O, pH 13): 22.31; **^{1}H NMR**: 0.72 (t, $^3J_{HH}$ = 7.2, $CH_3(CH_2)_5$, 3H), 0.93–1.22 (m, $CH_3(CH_2)_4CH_2$, 8H), 1.44–1.1.58 (m, $CH_3(CH_2)_4CH_2$, 2H), 2.90 (dd, $^3J_{HP}$ = 9.1, $^2J_{HH}$ = 14.0, PyCHHC, 1H), 3.52 (dd, $^3J_{HP}$ = 7.3, $^2J_{HH}$ = 14.0, PyCHHC, 1H), 7.27 (dd, $^3J_{HH}$ = 7.9, 4.8, $CH_{Ar\,(5)}$, 1H), 7.75 (dt, $^3J_{HH}$ = 7.9, $^4J_{HH}$ = 1.9, $CH_{Ar\,(4)}$, 1H), 8.25 (d, $^3J_{HH}$ = 4.8, $CH_{Ar\,(6)}$, 1H), 8.36 (s, $CH_{Ar\,(2)}$, 1H); **^{13}C NMR**: 11.57 (s, $CH_3(CH_2)_5$, 1C), 20.13, 27.94, 29.19 (3s, $CH_3(CH_2)_3(CH_2)_2$, 3C), 23.61 (d, $^3J_{CP}$ = 5.2, $CH_3(CH_2)_3CH_2CH_2$, 1C), 31.25 (s, $CH_3(CH_2)_4CH_2$, 1C), 35.30 (s, PyCH$_2$C, 1C), 53.45 (d, $^1J_{CP}$ = 115.3, C, 1C), 121.67 (s, $CH_{Ar\,(5)}$,1C), 135.66 (d, $^3J_{CP}$ = 14.9, $C_{Ar\,(3)}$, 1C), 137.15 (s, $CH_{Ar\,(4)}$,1C), 143.85 (s, $CH_{Ar\,(6)}$, 1C), 148.17 (s, $CH_{Ar\,(2)}$, 1C), 180.58 (s, C=O, 1C). **Elemental analysis**: $C_{14}H_{22}NO_5P(C_2H_5OH)_{0.19}$ Calculated: C 53.30, H 7.20, N 4.32; Found: C 53.36, H 7.12, N 4.32. **Scale**: **31g** (0.3 mmol), 0.12 g; **Yield**: 36%.

*5.1.13. 2-Phosphono-2-(pyridin-3-ylmethyl)decanoic acid (**1h**)*

^{31}P NMR (D_2O, pH 13): 22.05; **^{1}H NMR**: 0.82 (t, $^3J_{HH}$ = 7.1, $CH_3(CH_2)_7$, 3H), 0.97–1.22 (m, $CH_3(CH_2)_7CH_2$, 12H), 1.50–1.1.65 (m, $CH_3(CH_2)_6CH_2$, 2H), 2.95 (dd, $^3J_{HP}$ = 9.0, $^2J_{HH}$ = 14.1, PyCHHC, 1H), 3.58 (dd, $^3J_{HP}$ = 7.4, $^2J_{HH}$ = 14.1, PyCHHC, 1H), 7.30 (dd, $^3J_{HH}$ = 7.8, $^3J_{HH}$ = 4.9, $CH_{Ar\,(5)}$, 1H), 7.69 (d, $^3J_{HH}$ = 7.8, $CH_{Ar\,(4)}$, 1H), 8.16 (d, $^3J_{HH}$ = 4.9, $CH_{Ar\,(6)}$, 1H), 8.27 (s, $CH_{Ar\,(2)}$, 1H); **^{13}C NMR**: 11.59 (s, $CH_3(CH_2)_7C$, 1C), 20.17, 26.59, 26.77, 28.21, 29.33 (5s, $CH_3(CH_2)_5(CH_2)_2$, 5C), 23.59 (d, $^3J_{CP}$ = 5.3, $CH_3(CH_2)_5CH_2CH_2$, 1C), 31.16 (s, $CH_3(CH_2)_6CH_2$, 1C), 35.13 (s, PyCH$_2$C, 1C), 53.37 (d, $^1J_{CP}$ = 115.1, C, 1C), 121.68 (s, $CH_{Ar\,(5)}$, 1C), 135.85 (d, $^3J_{CP}$ = 14.8, $C_{Ar\,(3)}$, 1C), 137.15 (s, $CH_{Ar\,(4)}$, 1C), 143.83 (s, $CH_{Ar\,(6)}$, 1C), 148.19 (s, $CH_{Ar\,(2)}$, 1C), 180.56 (s, C=O, 1C); **Elemental analysis**: $C_{16}H_{26}NO_5P$ Calculated: C 55.97, H 7.63, N 4.08; Found: C 55.82, H 7.84, N 4.08; **Scale**: **31h** (0.48 mmol, 0.2 g); **Yield**: 56%.

*5.1.14. 2-(Imidazo[1,2-a]pyridin-3-ylmethyl)-2-phosphonooctanoic acid (**3g**)*

^{31}P NMR (D_2O, pH 13): 20.87; **^{1}H NMR**: 0.54–0.66 (m, $CH_3(CH_2)_5$, 3H), 0.77–1.00 (m, $CH_3(CH_2)_4CH_2$, 8H), 1.69–1.91 (m, $CH_3(CH_2)_4CH_2$, 2H), 3.22–3.31 (m, IPCHHC, 1H), 3.68–3.76 (m, IPCHHC, 1H), 6.95–7.01 (m, CH_{Ar}, 1H), 7.26–7.33 (m, CH_{Ar}, 1H), 7.37 (s, CH_{Ar}, 1H), 7.48–7.52 (m, CH_{Ar}, 1H), 8.42–8.46 (m, CH_{Ar}, 1H); **Scale**: **32g** (0.24 mmol, 0.1 g); **Yield**: 61%; (>93% purity).

5.2. Biological evaluations

5.2.1. FRET-biosensor assay on a flow cytometer

Screens were performed as described earlier [45,46]. In brief, BHK cells were transfected with either Rab5-, 8-, 21-NANOPS or Ras-NANOPS. Rab21-NANOPS with constitutively active form of Rab21 (Rab21Q76L) was constructed analogous to Rab5-NANOPS. 18 h after transfection cells were split to 96 well plates at 5×10^4 cells per well. After the cells have attached (usually 5–7 h), they were treated with the phosphonocarboxylate (PC) analogs at a final concentration of 500 μM for 24 h. All PC analogs were dissolved in PBS with pH 7.0–7.4 and stored in −20 °C until use. Following treatment, the cells were detached with 10 mM EDTA in PBS and fixed with equal volume of 4% PFA in PBS for 15 min at room temperature. All assays were performed as three independent experiments and each experiment had compactin as the internal control. Cytometry based FRET-measurements were made on a FACS LSR II (BD bioscience) using the following filters for donor- (405 nm excitation, 450/50 nm emission filter), acceptor- (488 nm, excitation, 585/42 nm emission filter) and FRET-channel (405 nm

excitation, 530/30 nm emission filter). The flow cytometer data were analysed as described earlier [60,61]. In brief, doublet discrimination was implemented to measure signals of single cells. For normalized acceptor level calibration, cA, FITC beads (Bangs Laboratories) with a defined size and fluorescein content were used as described. A mCFP–mCit fusion protein was used to calibrate for the FRET efficiency and donor–acceptor ratio. Only cells with a donor mole-fraction, $xD = 0.5 \pm 0.1$ were analysed. The Emax value was determined as described [45,46].

5.2.2. Confocal imaging

BHK cells were grown on coverslips, transfected using JetPRIME (Polyplus) for 24 h, treated with compounds for 24 h and fixed with 4% PFA (Sigma, #P6148) in PBS. The coverslips were mounted on microscopic slides using Mowiol 4–88 (Sigma, # 81381). A Zeiss LSM 510 confocal microscope with a 63×/1.4 oil DIC immersion objective was used to record 12 bit 512 × 512 fluorescent images, using 200 μm pinhole size and 0.09 μm pixel size in the frame mode with 8× averaging. The images were later processed in ImageJ.

5.2.3. Statistical analysis

Statistical differences between mean values of inhibitor treated and untreated samples were analysed using one-way ANOVA followed by Dunnett's test in GraphPad Prism (version 6.0b). Confidence *p*-levels are indicated by asterisks, with * denoting p, 0.05, ** denoting p, 0.01, and *** denoting p, 0.001. The mean IC_{50} values for inhibition were calculated from six measurements and data were analysed in GraphPad Prism by nonlinear regression analysis on log (inhibitor concentration) vs. normalized response with a Hill Slope of −1.0 using the Marquardt method.

5.2.4. Assessment of inhibition of prenylation by western blotting

The effects of the PC analogues on protein prenylation was studied using triton X-114 fractionation, in which prenylated proteins partition into the detergent-rich phase, whereas unprenylated proteins remain in the aqueous phase [62]. Briefly, Hela cells were seeded in DMEM into 12-well plates at 7×10^4 cells/well, then treated the following day with PCs in fresh medium. 48 h later (unless stated otherwise), cell monolayers were rinsed in PBS and lysed in 20 mM Tris, 150 mM NaCl, pH 7.5, 1% triton X-114, a sample taken for determination of protein concentration, then remaining lysate incubated at 37 °C for 10 min. Following centrifugation at 13,000 g for 2 min, the aqueous and detergent-rich phases were separated, then triton X-114 added back to the aqueous phase to 1% v/v and the extraction process repeated. Aqueous phases, equivalent to 20 mg of unfractionated lysate, were electrophoresed on 12% gels and western blotted for Rab11 (an abundant, ubiquitous Rab), β-actin, or unprenylated Rap1A, and bands detected using a LI-COR Odyssey Infrared Imager. Values quoted in the table are the lowest effective dose (from 3 independent experiments), i.e. the lowest dose at which unprenylated Rap1A or Rab11 was detected.

5.2.5. Assessment of cell viability using Alamar blue

The number of viable Hela cells following treatment with PC compounds for 72 h was assessed as previously described [7]. Briefly, Hela cells were seeded in 96 well plates at 5×10^3 cells/well, then treated the following day with PCs and BPs in replicates of 3. The data expressed are the mean ± SEM of at least 4 independent experiments.

5.2.6. GGPP synthase assays

GGPP synthase was purified and assayed as described [63]. Briefly, compounds under investigation were pre-incubated with 4 pmol GGPPS for 10 min, then the reaction initiated by adding 20 μl substrate containing 50 μM [1–14C] IPP (4 μCi/mmol) and 50 μM FPP. After 10 min, the assay was terminated by adding 200 μl 1:4 conc. HCl/Methanol. Reaction products were then extracted with 0.4 mL scintillation fluid (Microscint E, Perkin Elmer) and radioactivity in the upper phase determined by scintillation counting. Data was analysed using Graphpad Prism.

Acknowledgement

KMB is grateful for financial support provided by Ministry of Science and Higher Education in Poland (N N204 519839 and IP2010 003070). FPC is grateful for financial support from the Alliance for Better Bone Health. AKN is grateful for support by the graduate school, National Doctoral Programme in Informational and Structural Biology (ISB). This work was supported by the Academy of Finland (252381) fellowship grant, the Sigrid Juselius Foundation, the Cancer Society of Finland and the Marie-Curie Reintegration Grant to DA.

The authors thank Prof. Tadeusz Gajda and Prof. Charles E. McKenna for helpful discussions, Ms. Marzena Kujawa for technical assistance, Jonna Alanko for cloning of the Rab21-NANOPS.

Appendix A. Supporting information

Supplementary data related to this article can be found at http://dx.doi.org/10.1016/j.ejmech.2014.06.062.

References

[1] C.E. McKenna, L.A. Khawli, A. Bapat, V. Harutunian, Y. Chi Cheng, Inhibition of herpesvirus and human DNA polymerases by α-halogenated phosphonoacetates, Biochem. Pharmacol. 36 (1987) 3103–3106.
[2] C.E. McKenna, J.N. Levy, L.A. Khawli, V. Harutunian, T. Gao Ye, M.C. Starnes, A. Bapat, Y. Chi Cheng, Inhibitors of viral nucleic acid polymerases. pyrophosphate analogs, ACS Symp. Ser. 401 (1989) 1–16.
[3] S. Debarge, J. Balzarini, A.R. Maguire, Design and synthesis of α-carboxy phosphono-nucleosides, J. Org. Chem. 76 (2011) 105–126.
[4] M.S. Marma, Z.D. Xia, C. Stewart, F. Coxon, J.E. Dunford, R. Baron, B.A. Kashemirov, F.H. Ebetino, J.T. Triffitt, R.G.G. Russell, C.E. McKenna, Synthesis and biological evaluation of alpha-halogenated bisphosphonate and phosphonocarboxylate analogues of risedronate, J. Med. Chem. 50 (2007) 5967–5975.
[5] O.I. Artyushin, S.N. Osipov, G.-V. Röschenthaler, I.L. Odinets, Propargyl-substituted phosphonocarboxylates: efficient synthesis and application to click chemistry, Synthesis (2009) 3579–3588.
[6] F.H. Ebetino, A.-M.L. Hogan, S. Sun, M.K. Tsoumpra, X. Duan, J.T. Triffitt, A.A. Kwaasi, J.E. Dunford, B.L. Barnett, U. Oppermann, M.W. Lundy, A. Boyde, B.A. Kashemirov, C.E. McKenna, R.G.G. Russell, The relationship between the chemistry and biological activity of the bisphosphonates, Bone 49 (2011) 20–33.
[7] F.P. Coxon, M.H. Helfrich, B. Larijani, M. Muzylak, J.E. Dunford, D. Marshall, A.D. McKinnon, S.A. Nesbitt, M.A. Horton, M.C. Seabra, F.H. Ebetino, M.J. Rogers, Identification of a novel phosphonocarboxylate inhibitor of Rab geranylgeranyl transferase that specifically prevents Rab prenylation in osteoclasts and macrophages, J. Biol. Chem. 276 (2001) 48213–48222.
[8] F.H. Ebetino, A.V. Bayless, J. Amburgey, K.J. Ibbotson, S. Dansereau, A. Ebrahimpour, Elucidation of a pharmacophore for the bisphosphonate mechanism of bone antiresorptive activity, Phosphorus Sulfur Silicon Relat. Elem. 109–110 (1996) 217–220.
[9] A.J. Roelofs, P.A. Hulley, A. Meijer, F.H. Ebetino, R.G.G. Russell, C.M. Shipman, Selective inhibition of Rab prenylation by a phosphonocarboxylate analogue of risedronate induces apoptosis, but not S-phase arrest, in human myeloma cells, Int. J. Cancer 119 (2006) 1254–1261.
[10] P.G.J. Fournier, F. Dauhine, M.W. Lundy, M.J. Rogers, F.H. Ebetino, P. Clezardin, Lowering bone mineral affinity of bisphosphonates as a therapeutic strategy to optimize skeletal tumor growth inhibition in vivo, Cancer Res. 68 (2008) 8945–8953.
[11] C.E. McKenna, B.A. Kashemirov, K.M. Błażewska, I. Mallard-Favier, C.A. Stewart, J. Rojas, M.W. Lundy, F.H. Ebetino, R.A. Baron, J.E. Dunford, M.L. Kirsten, M.C. Seabra, J.L. Bala, M.S. Marma, M.J. Rogers, F.P. Coxon, Synthesis, chiral high performance liquid chromatographic resolution and enantiospecific activity of a potent new geranylgeranyl transferase inhibitor, 2-hydroxy-3-imidazo[1,2-a]pyridin-3-yl-2-phosphonopropionic acid, J. Med. Chem. 53 (2010) 3454–3464.
[12] K.M. Błażewska, F. Ni, R. Haiges, B.A. Kashemirov, F.P. Coxon, C.A. Stewart, R. Baron, M.J. Rogers, M. Seabra, F.H. Ebetino, C.E. McKenna, Synthesis,

stereochemistry and SAR of a series of minodronate analogues as RGGT inhibitors, Eur. J. Med. Chem. 46 (2011) 4820–4826.
[13] E.E. Kelly, C.P. Horgan, B. Goud, M.W. McCaffrey, The Rab family of proteins: 25 years on, Biochem. Soc. Trans. 40 (2012) 1337–1347.
[14] C. Recchi, M.C. Seabra, Novel functions for Rab GTPases in multiple aspects of tumour progression, Biochem. Soc. Trans. 40 (2012) 1398–1403.
[15] J.D. Ochocki, M.D. Distefano, Prenyltransferase inhibitors: treating human ailments from cancer to parasitic infections, MedChemComm 4 (2013) 476–492.
[16] Z. Guo, Y.W. Wu, K.T. Tan, R.S. Bon, E. Guiu-Rozas, C. Delon, U.T. Nguyen, S. Wetzel, S. Arndt, R.S. Goody, W. Blankenfeldt, K. Alexandrov, H. Waldmann, Development of selective RabGGTase inhibitors and crystal structure of a RabGGTase-inhibitor complex, Angew. Chem. Int. Ed. 47 (2008) 3747–3750.
[17] K.-T. Tan, E. Guiu-Rozas, R.S. Bon, Z. Guo, C. Delon, S. Wetzel, S. Arndt, K. Alexandrov, H. Waldmann, R.S. Goody, Y.-W. Wu, W. Blankenfeldt, Design, synthesis, and characterization of peptide-based Rab geranylgeranyl transferase inhibitors, J. Med. Chem. 52 (2009) 8025–8037.
[18] M. Watanabe, H.D.G. Fiji, L. Guo, L. Chan, S.S. Kinderman, D.J. Slamon, O. Kwon, F. Tamanoi, Inhibitors of protein geranylgeranyltransferase I and Rab geranylgeranyltransferase identified from a library of allenoate-derived compounds, J. Biol. Chem. 283 (2008) 9571–9579.
[19] R.S. Bon, Z. Guo, E. Anouk Stigter, S. Wetzel, S. Menninger, A. Wolf, A. Choidas, K. Alexandrov, W. Blankenfeldt, R.S. Goody, H. Waldmann, Structure-guided development of selective RabGGTase inhibitors, Angew. Chem. Int. Ed. 50 (2011) 4957–4961.
[20] C. Deraeve, Z. Guo, R.S. Bon, W. Blankenfeldt, R. DiLucrezia, A. Wolf, S. Menninger, E. Anouk Stigter, S. Wetzel, A. Choidas, K. Alexandrov, H. Waldmann, R.S. Goody, Y.-W. Wu, Psoromic acid is a selective and covalent Rab-prenylation inhibitor targeting autoinhibited RabGGTase, J. Am. Chem. Soc. 134 (2012) 7384–7391.
[21] X. Zhou, S.V. Hartman, E.J. Born, J.P. Smits, S.A. Holstein, D.F. Wiemer, Triazole-based inhibitors of geranylgeranyltransferase II, Bioorg. Med. Chem. Lett. 23 (2013) 764–766.
[22] R.A. Baron, R. Tavaré, A.C. Figueiredo, K.M. Błażewska, B.A. Kashemirov, C.E. McKenna, F.H. Ebetino, A. Taylor, M.J. Rogers, F.P. Coxon, M.C. Seabra, Phosphonocarboxylates inhibit the second geranylgeranyl addition by Rab geranylgeranyl transferase, J. Biol. Chem. 284 (2009) 6861–6868.
[23] J. Hwan No, F. De Macedo Dossin, Y. Zhang, Y.-L. Liu, W. Zhu, X. Feng, J. Anny Yoo, E. Lee, K. Wang, R. Hui, L.H. Freitas-Junior, E. Oldfield, Lipophilic analogs of zoledronate and risedronate inhibit Plasmodium geranylgeranyl diphosphate synthase (GGPPS) and exhibit potent antimalarial activity, Proc. Natl. Assoc. Sci. U. S. A. 109 (2012) 4058–4063.
[24] B. Fiszer, J. Michalski, Synthesis of organophosphorus compounds based on phosphonoacetic ester and its analogs. Addition of phosphonoacetic ester, alkylated phosphonoacetic esters, and phosphonoacetic nitrile to α, β-unsaturated esters and nitriles, Rocz. Chem. 28 (1954) 185–195.
[25] K. Lee, D.F. Wiemer, A convenient preparation of α-phosphono esters and lactones via carbon-phosphorus bond formation, Phosphorus Sulfur Silicon Relat. Elem. 75 (1993) 87–90.
[26] H. Krawczyk, K. Wąsek, J. Kędzia, J. Wojciechowski, W.M. Wolf, A general stereoselective method for the synthesis of cyclopropanecarboxylates. A new version of the homologous Horner-Wadsworth-Emmons reaction, Org. Biomol. Chem. 6 (2008) 308–318.
[27] P. Coutrot, A. Ghribi, A facile and general one-pot synthesis of 2-oxoalkanephosphonates from diethylphosphonocarboxylic acid chlorides and organometallic reagents, Synthesis (1986) 661–664.
[28] K. Hackelöer, G. Schnakenburg, S.R. Waldvogel, Oxidative coupling reactions of 1,3-diarylpropene derivatives to dibenzo[a,c]cycloheptenes by PIFA, Eur. J. Org. Chem. 2011 (2011) 6314–6319.
[29] E. Błaszczyk, H. Krawczyk, T. Janecki, 2-Diethoxyphosphoryl-4-nitroalkanoates – versatile intermediates in the synthesis of α-alkylidene-γ-lactones and lactams, Synlett (2004) 2685–2688.
[30] L. Albrecht, B. Richter, H. Krawczyk, K. Anker Jørgensen, Enantioselective organocatalytic approach to α-methylene-δ-lactones and δ-lactams, J. Org. Chem. 73 (2008) 8337–8343.
[31] F.H. Ebetino, A.V. Bayless, S.M. Dansereau, Phosphonocarboxylate compounds pharmaceutical compositions, and methods for treating abnormal calcium and phosphate metabolism, The Procter and Gamble Co., USA, US Patent 5,760,021, 1998.
[32] J.N. Levy, C.E. McKenna, Oxidations of triethyl a-phosphonoacrylate. Epoxidation to triethyl a-phosphonoacrylate oxide by hypochlorite and formation of triethyl dihydroxyphosphonoacetate with RuO_4-periodate, Phosphorus Sulfur Silicon Relat. Elem. 85 (1993) 1–8.
[33] B. Iorga, F. Eymery, P. Savignac, The synthesis and properties of 1,2-epoxyalkylphosphonates, Synthesis (1999) 207–224.
[34] F.M.D. Ismail, Important fluorinated drugs in experimental and clinical use, J. Fluor. Chem. 118 (2002) 27–33.
[35] S. Purser, P.R. Moore, S. Swallow, V. Gouverneur, Fluorine in medicinal chemistry, Chem. Soc. Rev. 37 (2008) 320–330.
[36] I. Ojima, Exploration of fluorine chemistry at the multidisciplinary interface of chemistry and biology, J. Org. Chem. 78 (2013) 6358–6383.
[37] J. Wang, M. Sánchez-Roselló, J.L. Aceña, P. Carlos del, A.E. Sorochinsky, S. Fustero, V.A. Soloshonok, H. Liu, Fluorine in pharmaceutical industry: fluorine-containing drugs introduced to the market in the last decade (2001–2011), Chem. Rev. 114 (2014) 2432–2506.
[38] K.M. Błażewska, R. Haiges, B.A. Kashemirov, F.H. Ebetino, C.E. McKenna, A serendipitous phosphonocarboxylate complex of boron: when vessel becomes reagent, Chem. Commun. 47 (2011) 6395–6397.
[39] M.S. Marma, L.A. Khawli, V. Harutunian, B.A. Kashemirov, C.E. McKenna, Synthesis of alpha-fluorinated phosphonoacetate derivatives using electrophilic fluorine reagents: perchloryl fluoride versus 1-chloromethyl-4-fluoro-1,4-diazoniabicyclo[2.2.2]octane bis(tetrafluoroborate) (selectfluor (R)), J. Fluor. Chem. 126 (2005) 1467–1475.
[40] Y.-S. Lin, J. Park, Joris W. De Schutter, X. Fang Huang, A.M. Berghuis, M. Sebag, Y.S. Tsantrizos, Design and synthesis of active site inhibitors of the human farnesyl pyrophosphate synthase: apoptosis and inhibition of ERK phosphorylation in multiple myeloma cells, J. Med. Chem. 55 (2012) 3201–3215.
[41] M.F. Semmelhack, J.C. Tomesch, M. Czarny, S. Boettger, Preparation of 2-(alkylthiomethyl)acrylates, J. Org. Chem. 43 (1978) 1259–1262.
[42] W.J. Kruper Jr., P.R. Rudolf, C.A. Langhoff, Unexpected selectivity in the alkylation of polyazamacrocycles, J. Org. Chem. 58 (1993) 3869–3876.
[43] T. Nagata, M. Inoue, Y. Ashida, K. Noguchi, M. Ono, 3-(3-Cycloalkyl-1H-imidazol-4-yl)propanoic acid derivatives as inhibitors of thrombin-activatable fibrinolysis inhibitor (TAFIa), PCT Int. Appl. WO2011115064A1, 2011.
[44] Procedure applied from: N. Camper, Ch. Scott, M.E. Migaud, Synthesis of an analogue of the bisphosphonate drug ibandronate for targeted drug-delivery therapeutic strategies New J. Chem. 34 (2010) 949–955.
[45] M. Köhnke, S. Schmitt, N. Ariotti, A.M. Piggott, R.G. Parton, E. Lacey, R.J. Capon, K. Alexandrov, D. Abankwa, Design and application of in vivo FRET biosensors to identify protein prenylation and nanoclustering inhibitors, Chem. Biol. Oxf. U. K. 19 (2012) 866–874.
[46] A.K. Najumudeen, M. Köhnke, M. Šolman, K. Alexandrov, D. Abankwa, Cellular FRET-biosensors to detect membrane targeting inhibitors of N-myristoylated proteins, PLoS One 8 (2013) e66425.
[47] J.E. Dunford, K. Thompson, F.P. Coxon, S.P. Luckman, F.M. Hahn, C. Dale Poulter, F.H. Ebetino, M.J. Rogers, Structure-activity relationships for inhibition of farnesyl diphosphate synthase in vitro and inhibition of bone resorption in vivo by nitrogen-containing bisphosphonates, J. Pharmacol. Exp. Ther. 296 (2001) 235–242.
[48] A. Dudakovic, A.J. Wiemer, K.M. Lamb, L.A. Vonnahme, S.E. Dietz, R.J. Hohl, Inhibition of geranylgeranyl diphosphate synthase induces apoptosis through multiple mechanisms and displays synergy with inhibition of other isoprenoid biosynthetic enzymes, J. Pharmacol. Exp. Ther. 324 (2008) 1028–1036.
[49] A.J. Wiemer, R.J. Hohl, D.F. Wiemer, The intermediate enzymes of isoprenoid metabolism as anticancer targets, Anti Cancer Agents Med. Chem. 9 (2009) 526–542.
[50] F.P. Coxon, M.H. Helfrich, H. Robert Van't, S. Sebti, S.H. Ralston, A. Hamilton, M.J. Rogers, Protein geranylgeranylation is required for osteoclast formation, function, and survival: Inhibition by bisphosphonates and GGTI-298, J. Bone Min. Res. 15 (2000) 1467–1476.
[51] F.P. Coxon, A. Taylor, C.A. Stewart, R. Baron, M.C. Seabra, F.H. Ebetino, M.J. Rogers, The gunmetal mouse reveals Rab geranylgeranyl transferase to be the major molecular target of phosphonocarboxylate analogues of bisphosphonates, Bone 49 (2011) 111–121.
[52] C.M. Szabo, Y. Matsumura, S. Fukura, M.B. Martin, J.M. Sanders, S. Sengupta, J.A. Cieslak, T.C. Loftus, C.R. Lea, H.-J. Lee, A. Koohang, R.M. Coates, H. Sagami, E. Oldfield, Inhibition of geranylgeranyl diphosphate synthase by bisphosphonates and diphosphates: a potential route to new bone antiresorption and antiparasitic agents, J. Med. Chem. 45 (2002) 2185–2196.
[53] K.-M.C. Cammy, M.P. Hudock, Y. Zhang, R.-T. Guo, R. Cao, J.H. No, P.-H. Liang, T.-P. Ko, T.-H. Chang, S.-c. Chang, Y. Song, J. Axelson, A. Kumar, A.H.-J. Wang, E. Oldfield, Inhibition of geranylgeranyl diphosphate synthase by bisphosphonates: a crystallographic and computational investigation, J. Med. Chem. 51 (2008) 5594–5607.
[54] R.J. Barney, B.M. Wasko, A. Dudakovic, R.J. Hohl, D.F. Wiemer, Synthesis and biological evaluation of a series of aromatic bisphosphonates, Bioorg. Med. Chem. 18 (2010) 7212–7220.
[55] U.T.T. Nguyen, J. Cramer, J. Gomis, R. Reents, M. Gutierrez-Rodriguez, R.S. Goody, K. Alexandrov, H. Waldmann, Exploiting the substrate tolerance of farnesyltransferase for site-selective protein derivatization, ChemBioChem 8 (2007) 408–423.
[56] Z. Guo, Y.W. Wu, D. Das, C. Delon, J. Cramer, S. Yu, S. Thuns, N. Lupilova, H. Waldmann, L. Brunsveld, R.S. Goody, K. Alexandrov, W. Blankenfeldt, Structures of RabGGTase-substrate/product complexes provide insights into the evolution of protein prenylation, EMBO J. 27 (2008) 2444–2456.
[57] A.Q. Gomes, B.R. Ali, J.S. Ramalho, R.F. Godfrey, D.C. Barral, A.N. Hume, M.C. Seabra, Membrane targeting of Rab GTPases is influenced by the prenylation motif, Mol. Biol. Cell. 14 (2003) 1882–1899.
[58] U.T.T. Nguyen, A. Goodall, K. Alexandrov, D. Abankwa, Isoprenoid modifications, Protein Rev. Post Transl. Modifi. Health Dis. 13 (2011) 1–37.
[59] N.H. Thomä, A. Iakovenko, D. Owen, A.S. Scheidig, H. Waldmann, R.S. Goody, K. Alexandrov, Phosphoisoprenoid binding specificity of geranylgeranyltransferase type II, Biochemistry 39 (2000) 12043–12052.
[60] D. Abankwa, H. Vogel, A FRET map of membrane anchors suggests distinct microdomains of heterotrimeric G proteins, J. Cell. Sci. 120 (2007) 2953–2962.
[61] D. Abankwa, M. Hanzal-Bayer, N. Ariotti, S.J. Plowman, A.A. Gorfe, R.G. Parton, J. Andrew McCammon, J.F. Hancock, A novel switch region regulates H-ras membrane orientation and signal output, EMBO J. 27 (2008) 727–735.

[62] F.P. Coxon, F.H. Ebetino, E.H. Mules, M.C. Seabra, C.E. McKenna, M.J. Rogers, Phosphonocarboxylate inhibitors of Rab geranylgeranyl transferase disrupt the prenylation and membrane localization of Rab proteins in osteoclasts in vitro and in vivo, Bone 37 (2005) 349–358.

[63] K.L. Kavanagh, K. Guo, J.E. Dunford, X. Wu, S. Knapp, F.H. Ebetino, M.J. Rogers, R.G.G. Russell, U. Oppermann, The molecular mechanism of nitrogen-containing bisphosphonates as antiosteoporosis drugs, Proc. Natl. Assoc. Sci. U. S. A. 103 (2006) 7829–7834.